

A step towards the integration of spatial dynamics in population dynamics models: Eastern Bering Sea snow crab as a case study



Maxime Olmos^{a,b,1,*}, Jie Cao^c, James T. Thorson^b, André E. Punt^a, Cole C. Monnahan^b, Baptiste Alglave^a, Cody Szuwalski^b

^a School of Aquatic and Fishery Sciences, University of Washington, Seattle, WA, USA

^b Alaska Fisheries Science Center, National Marine Fisheries Service, NOAA, Seattle, WA, USA

^c Department of Applied Ecology, North Carolina State University, Morehead City, NC, USA

ARTICLE INFO

Keywords:

Chionoecetes opilio
Size-structured spatiotemporal model
Spatial management
State-space model

ABSTRACT

Considering spatial processes in population dynamics models can be difficult because of data limitations and computational costs. We adapted a high-resolution spatiotemporal assessment framework to better address fine-scale spatial heterogeneities based on theories of fish population dynamics and spatiotemporal statistics. Specifically, we developed a size-based state-space model for the snow crab (*Chionoecetes opilio*) population in the Eastern Bering Sea (EBS) to refine the representation of spatial processes in integrated population models, facilitate understanding of the drivers of spatiotemporal population dynamics, and provide new insights for management advice. The model fits to spatial survey and fishery-dependent catch data. It implicitly accounts for seasonal movement between the time of the survey and that of fishery to estimate fine-scale spatial population dynamic and fishing impacts, including potential environmental drivers. We quantify, for the first time, spatiotemporal variation in exploitable abundance, fishing mortality, recruitment, and mature and immature abundance. The model estimated declines in exploitable abundance and in fishing mortality with variable spatial distributions, and sporadic recruitment, spatially concentrated in the northeast EBS. Few spatial assessments have been used as the basis for management advice and we consider this study as a step towards the integration of spatial dynamics in stock assessment.

1. Introduction

Modeling spatiotemporal dynamics is a challenge for understanding ecological drivers of populations, but considering spatial processes in population dynamics models can be difficult because of data limitations and computational costs (Punt, 2019). In fisheries science, population dynamics models ("stock assessments") are used to provide management advice (Walters and Martell, 2004), and accounting for spatially explicit processes in stock assessments has been identified as an essential feature of next generation stock assessment models (Cadrin, 2020; Punt et al., 2020). Single-species population dynamics models driven by reproduction, growth, maturation, fishing, natural mortality and recruitment, are common stock assessment models (Hilborn and Walters, 1992; Quinn and Deriso, 1999). But most fisheries stock assessment models make implicit assumptions about spatial processes by considering the population and the key demographic features driving the population

dynamics as homogeneously distributed across space. However, ignoring spatial structure in population dynamics models can lead to bias in estimated quantities needed for management (Punt, 2019) and limits our understanding of the mechanisms driving the spatiotemporal dynamics of populations (Rogers et al., 2017).

Spatially explicit integrated population models (IPMs) are becoming popular as they can integrate several data sources to infer shared ecological processes between the data sources (here spatially varying demographic processes - Maunder and Punt, 2013; Berger et al., 2017). Spatial IPMs can be separated into two categories: spatially stratified and spatiotemporal IPMs. Spatially stratified models divide the spatial domain into independent subareas (i.e., spatial strata), where connectivity is either estimated or specified as instantaneous movement among areas (Goethel et al., 2011; Szuwalski and Punt, 2015). Spatially stratified models have numerous limitations. For instance, these models require a good knowledge of stock spatial structure which is not the case

* Corresponding author.

E-mail address: maxime.olmos@ifremer.fr (M. Olmos).

¹ Present address: DECOD (Ecosystem Dynamics and Sustainability), IFREMER, INRAE, Institut Agro, ZI Pointe du Diable, Plouzane F-29,280, France.

for many stocks. Furthermore, they still assume homogenous dynamics within each stock subunit, which can be an unrealistic assumption.

In contrast, spatiotemporal IPMs are implemented at a finer spatial scale than spatially stratified models. They reproduce population dynamics using similar equations to spatially stratified model but also account for the spatio-temporal correlation processes occurring at fine scale (Kristensen et al., 2014; Thorson et al., 2015, 2017; Cadigan et al., 2017; Cao et al., 2020; McDonald et al., 2021). Furthermore, non-spatial stock assessments involve creating aggregated abundance indices based on survey data. In contrast, spatiotemporal IPMs can directly fit survey data at the scale they were collected attribute variation in monitoring data among sampling locations to sampling error and spatial process heterogeneity (Thorson and Haltuch, 2019). In particular, one advantage of spatiotemporal model is to inform spatiotemporal locations with few data based on the spatiotemporal correlation structure (Breivik et al., 2021). However, spatiotemporal models have large computational demands because they have many correlated random effects.

State-space spatiotemporal IPMs can account for measurement and process errors (Kristensen et al., 2014) and population dynamics can be built into the model (e.g., Thorson et al. (2015) delay-difference models). Thorson et al. (2017) and McDonald et al. (2021) developed a biomass dynamics spatiotemporal model and Cadigan et al. (2017) developed a CPUE and survey-integrated spatial biomass depletion model. These models usually do not account for many population processes, such as maturity, growth, or movement. Excluding these processes from models can make interpretation and understanding of population processes difficult. Refining the way in which population processes are modeled in spatiotemporal IPMs is a key challenge for improving their realism.

Cao et al. (2020) developed a spatially explicit IPM in a state-space framework to account for fine-scale spatial heterogeneity in population dynamics. This framework allows spatial patterns in the key quantities for management such as fishing mortality, recruitment, mature and immature abundance and spawning stock abundance to be estimated. It opens the gate for the possibility of a novel generation of stock assessment methods that account for the spatio-temporal dimension of population dynamics (Punt et al., 2020).

Nevertheless, whether state-space spatially-explicit IPMs can be applied for production stock assessment purposes remains an open question because Cao et al. (2020) used only simulated data within a proof-of-concept analysis. Moving from simulated to real data is a crucial step in making this approach operational for management and

requires examination because the data may not be available in the controlled and well-designed configuration of a simulation. In this paper, we build on the Cao et al. (2020) framework and show its operational applicability by fitting the model to the data available for the snow crab (*Chionoecetes opilio*) in the Eastern Bering Sea (EBS). The snow crab fishery is an historically lucrative fishery in which fishers target only males and most exploitation occurs during winter (Szuwalski (2019); Fig. 1). Both fish abundance and fishery effort are characterized by strong spatial and temporal variability. Estimates of snow crab biomass declined markedly in 2021, with total mature and immature male biomass the lowest on record (Zacher et al., 2021). It has been hypothesized that the large fluctuations in abundance and catch might be due to variable recruitment (Kruse et al., 2007; Szuwalski et al., 2021), characterized by periodic pulses (Ernst et al., 2012) with possible link with the extent of the cold pool in the EBS (a subsurface mass of cold water (<2 °C) forming over the middle shelf each spring when sea ice retreats) (Mueter and Litzow, 2008). Fitting a spatio-temporal population dynamics model for snow crab could reveal key information on the spatio-temporal dynamics of the fishery and could provide additional insights in the recent modifications in population dynamics.

We developed a size- and stage-based state space model fitted on a fine scale spatial grid at a yearly time step for the years 1989–2018. As movement is a key demographic process for this case study (e.g. seasonal, ontogenetic, reproductive migration - Barbeaux and Hollowed, 2018; Fokkema et al., 2020), it is given special attention in the framework.

Ultimately, our model produces fine scale maps of exploitable abundance, mature and immature abundance, recruitment, and fishing mortality at the scale of the grid on which surveys are based. We use these model outputs to explore important questions in management such as the spatial distribution of fishing mortality and the effect of the cold pool on spatio-temporal variation in juvenile distribution.

2. Material and methods

Below, we describe the size-structured spatiotemporal model and list some challenges (and their solutions) arising from fitting the model to actual data for snow crab. It integrates fishery- and survey-catches-at-size and accounts for demographic processes using a size-class structure. The representation of several biological and sampling processes (e.g., selectivity, maturity, fishing mortality) is modeled more realistically than by Cao et al. (2020). Movement needed to be accounted for when

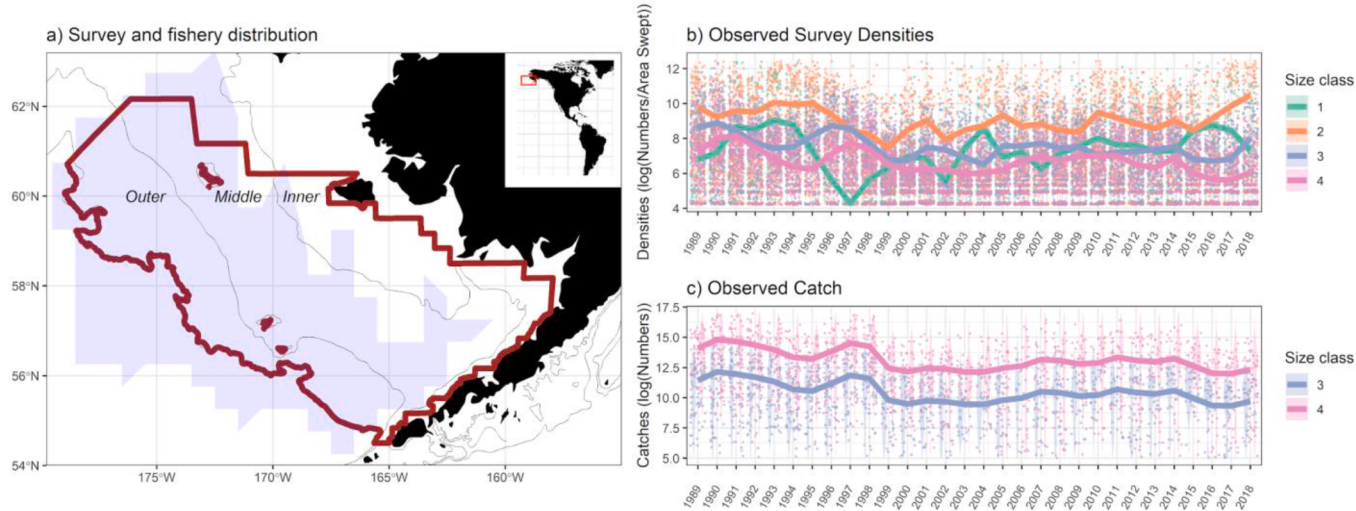


Fig. 1. a) Spatial footprint of the survey data (red polygon) and the fishery data (blue polygon), defined as the total area where crabs were harvested from 1989 to 2018. Annual observed survey densities (b) and fishery catches for size-classes 3 and 4 (c) (size-classes 1 and 2 are not caught). Dots in b) and c) represent individual trawls/pots across the spatial domain and medians are shown as lines.

fitting the model because the survey occurs during summer while fishing occurs during the following winter and snow crab conduct seasonal migrations between these two periods. Here we proposed to reconstruct the spatial distribution, during the summer survey, of fish that were later caught in the following winter fishery. As a first approach, we assume crabs migrate seasonally through a linear translation between when the survey takes place (summer) and when fishing occurs (in the following winter) and we account for possible diffusion processes during migration.

We represent matrices with bold uppercase notation and vectors with bold lowercase notation (Edwards & Auger-Méthé, 2019). To keep the presentation concise, most model equations and data sources are detailed in Supporting Information S1, and indices used in model descriptions, data, and estimated parameters are listed in Table SI.1.

2.1. A size-structured spatiotemporal state-space model

2.1.1. The spatiotemporal state-space model

The IPM is a state-space spatiotemporal model of abundance by size-class that accounts for process and observation stochasticity. It is defined over a discrete spatial grid (Fig. SI.1) on a yearly time step from 1989 to 2018. Following Cao et al. (2020), we defined $d_{t,s}(l)$ as the density of animals (with units numbers per square kilometer) in size-class l in cell s and time t , and specify $\mathbf{d}_{t+1,s} = (d_{s,t}(1), \dots, d_{s,t}(L))$. The state-space model assumes multiplicative process error (ϵ) where the density $\mathbf{d}_{t+1,s}$ is the product of a function $f(\mathbf{d}_{t,s})$ and a process error term $e^{\epsilon_{t,s}}$.

$$\mathbf{d}_{t+1,s} = f(\mathbf{d}_{t,s}) \circ e^{\epsilon_{t,s}} \quad (1)$$

where $f(\mathbf{d}_{t,s})$ is a function of the density during year t and the parameters describing the population dynamics. $\epsilon_{t,s}$ is a process error component to account for unmodelled life history processes in space and time and is modeled as random effects for each year t , size-class l and cell s . Process errors are assumed to follow a multivariate normal distribution

$$\text{vec}[\mathbf{E}_t] \sim MVNormal(\mathbf{R}_{\text{spatial}} \otimes \Theta_L) \quad (2)$$

where \mathbf{E}_t is a matrix composed of $\epsilon_{t,s}$ at every modeled cell s , in a given year t and for a size-class l . $\text{vec}[\mathbf{E}_t]$ is a vector composed of stacking every column of \mathbf{E}_t , $\mathbf{R}_{\text{spatial}}$ is the correlation matrix controlling spatial correlation in process errors, Θ_L is a 4 by 4 matrix of the pairwise covariance between any two size-classes, and \otimes denotes the Kronecker operator such that $\mathbf{R}_{\text{spatial}} \otimes \Theta_L$ is a covariance matrix between the error process components for any two size-class l and l' and between any two spatial locations s and s' . We calculated the cross-correlation matrix between size classes from the variance-covariance matrix Θ_L . More details about the parameters of the multivariate normal distribution can be found in Supp. Mat. I. (Eq. (SI.3, SI.4)).

2.1.2. Population dynamics

The model considers four size-classes: the first two size-classes (0–40 mm, 40–78 mm) are not subject to fishing-related mortality whereas the largest two size-classes (78–101 mm, >101 mm) are subject to harvest. The model tracks crab densities (i.e., numbers per km²) by spatial cell for each size-class and maturity state from 1989 to 2019 over the entire study area (i.e., the survey footprint, Fig. 1). The density $\mathbf{d}_{t,s} = (d_{t,s,1}, \dots, d_{t,s,L}, \dots, d_{t,s,L})$ over time t and space s (defined as a cell in Fig. SI.1), for the $L (=4)$ size classes is controlled by recruitment $\mathbf{r}_{t,s}$ over time and space (recruits only enter the first size class of the model; they are the smallest individuals that are being available by the survey), growth \mathbf{G} (individuals grow from one size-class to larger size-classes over time), natural mortality m , and fishing mortality at size $\mathbf{f}_{t,s}$ through Eq. (1). Maturity at size, \mathbf{w}_t , accounts for the proportion of immature individuals in size class l that mature during year t (snow crab do not grow once they mature). Note that, in Eq. (1), for mature fish, the second term accounts for mature individuals that no longer grow.

$$\mathbf{d}_{t,s} = \begin{cases} \mathbf{r}_{t,s} + G \times \mathbf{d}_{t-1,s} \times \exp(-m - \mathbf{f}_{t-1,s}) \times (1 - \mathbf{w}_t), & \text{if } d = \mathbf{d}^{\text{immature}} \\ G \times \mathbf{d}_{t-1,s} \times \exp(-m - \mathbf{f}_{t-1,s}) \times \mathbf{w}_t + \mathbf{d}_{t-1,s} \times \exp(-m - \mathbf{f}_{t-1,s}), & \text{if } d = \mathbf{d}^{\text{mature}} \end{cases} \quad (3)$$

Catch at size $\mathbf{c}_{t,s}$ (in number per km²) is modeled using Eq. (2).

$$\mathbf{c}_{t,s} = (1 - \exp(-\mathbf{f}_{t,s})) \times \mathbf{d}_{t,s} \times \exp(-m) \quad (4)$$

See Supp. Mat. I. for more details about the overall population dynamics model.

2.1.3. Accounting for movement and seasonality

The spatial distribution of the stock changes between the survey and the fishery because the survey and fishery do not take place at the same time, making it necessary to account for movement and seasonality when fitting the model to the data. To account for seasonal movement and to reconstruct the spatial distribution during the summer survey of fish that were later caught in the following winter fishery, we assume all individuals for a given size class and year experience the same directional displacement between winter and summer following a linear translation. This is achieved through several steps:

- 1) compute the centers of gravity of the winter commercial catches and summer scientific survey abundance data per size and year (Fig. 2.a for all years and Fig. 3.a for a specific year),
- 2) match the centroid of the fishery catch in winter with the centroid of the crab abundance the previous summer and make the translation of the catch while accounting for possible diffusion movement during migration (Fig. 3.b), and
- 3) aggregate the translated catch (defined by Alaska Department of Fish and Game units) at the level of the model discretization (Fig. 3.c).
- 4) account for natural mortality during seasonal migration

This procedure is further described and justified in Supp. Mat. I, section I.3.3.

2.2. Observation model

The likelihood function for the state-space model is based on the combination of all observation equations for the survey and fishery data for each year, location, and size class. Survey and fishery data and likelihoods are defined in Supp. Mat. I. Based on Thorson (2018) and similarly as Cao et al. (2020), we used a Poisson-link delta model for the survey data (Supp. Mat. I, eq. SI.8–9).

The number of crabs $C_{t,s,l}^{\text{obs}}$ by size-class caught by the fishery was used to estimate the spatial fishing mortality $f_{t,s,l}$. For the snow crab fishery in the EBS there is an observer program with high coverage few landing sites and monitoring of catches on offload (Gaeuman, 2014). Fishery catch have then very few uncertainties, so the catch $C_{t,s,l}^{\text{obs}}$ was assumed to be lognormally distributed, with a fixed variance (based on Cao et al. (2020), we assumed the observation error for the fishery catches had a coefficient of variation of 5%, i.e. $\sigma_{C_f}^2 = 0.05$).

2.3. Model parameters and estimation

The model estimates spatiotemporal variation in fishing mortality, exploitable abundances, recruitment, and mature and immature abundances at the level of each cell. We pre-specified the values governing some demographic processes (i.e. mature proportion, natural mortality, growth, survey selectivity, Supp. Mat. SI, Fig. SI.6–8, Table.S2) consistent with the actual assessment for EBS snow crab (Szwalski, 2019), and we estimated the remainder as fixed or random effects (Supp. Mat. section SI). Process error in crab density from the state space structure can account for numerous unmodelled life history processes in

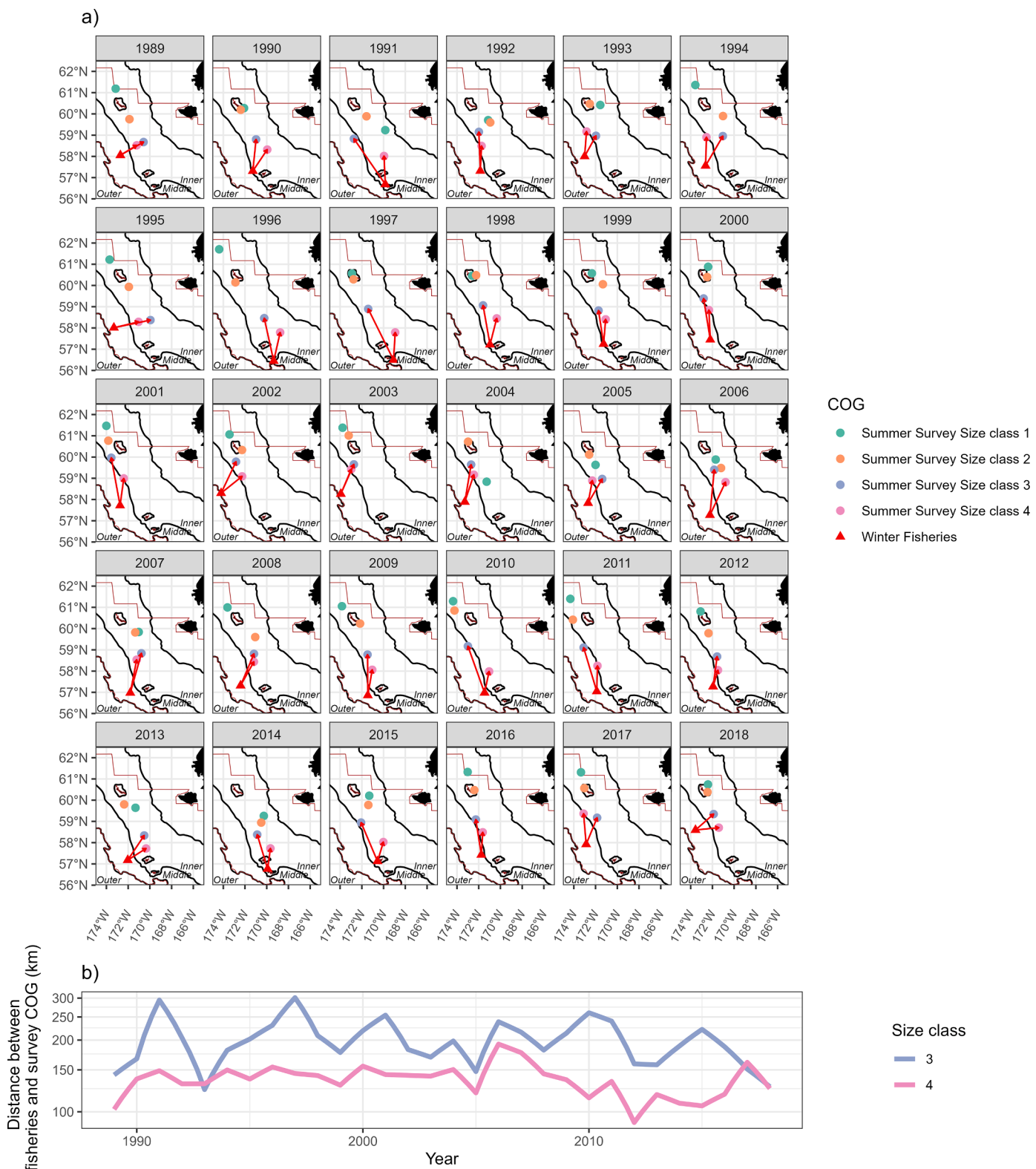


Fig. 2. a) Center of gravity (COG) of observed survey densities and observed fishery catches. Arrows represent movement between the survey and the fishery for size-classes 3 and 4. b) Distances between the survey and fishery COGs for size-classes 3 and 4.

spatiotemporal IPMs, including spatial and temporal variation in movement (other than the seasonal movement between the fishery and the survey, (e.g., southward ontogenetic migration of recruits), maturity, growth, and natural mortality).

2.3.1. Maximum likelihood estimation through TMB

Model estimation was realized through Maximum Likelihood Estimation within the TMB package (Template Model Builder - [Kristensen et al. \(2016\)](#)). TMB implements (1) Laplace approximation to evaluate the marginal likelihood, (2) fast computation techniques for sparse matrices and (3) Automatic Differentiation for fast computation of

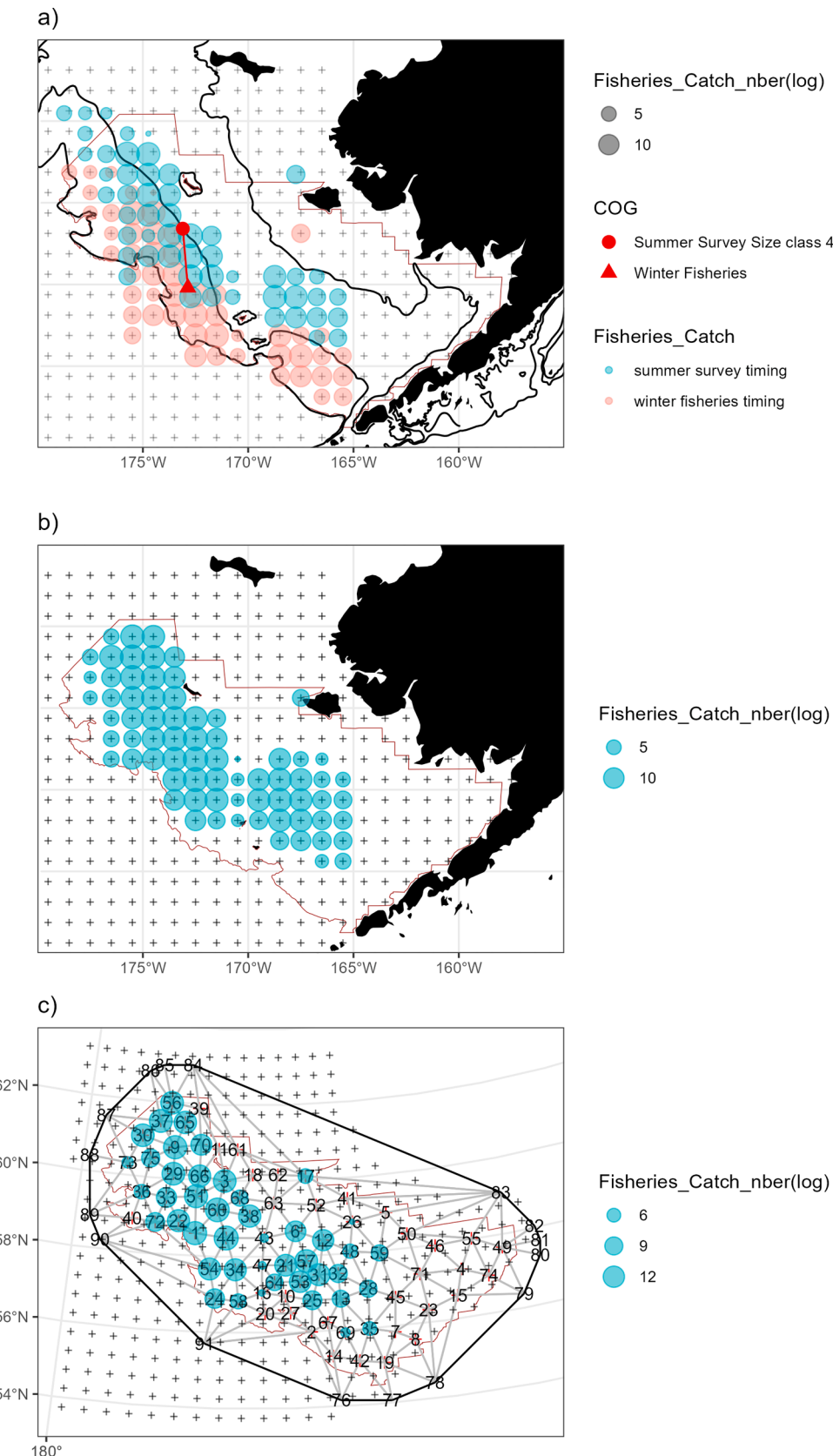


Fig. 3. Reconstruction of the spatial distribution of catches at the time of the survey (example for 2017, and size-class 4). (a) represents catches at the time of survey (in numbers, blue dots) after movement (represented by the distance between catch and survey COG, red line) has been reversed to each catch location.). Pink dots are catches at the time of fishing, red dot and triangle represent survey and catch centers of gravity respectively; grey crosses represent Alaska Department of Fish and Game (ADFG) cells. (b) Averaged catches across ADFG cells. We considered that the ADFG cells where crabs are harvested during the survey timing could be any of the four ADFG cells closest to the location they moved to, with the equal probability because we do not have any direct measurement of crab migratory behavior. We only included catches within the survey area in the model ($C_{t=2017,c,l=4}^{obs}$). (c) The process for aggregating catches to match the spatial resolution of the model. Catches from (a), which were indexed by ADFG cell, were allocated to the nearest knot and summed across knots. Further details of each step can be found in Figure SI.4.

derivatives. Standard errors are computed through the delta method.

2.3.2. Estimation of spatial random effects

We adopted the SPDE approach, which approximates continuous Gaussian fields with discrete Gaussian Markov random fields (Lindgren et al., 2011) to allow efficient estimation of the spatial random fields. This approach divides the discrete spatial domain (corresponding to the survey footprint, Fig. 1) composed of n_s discrete spatial cells s into a triangulated mesh created based on a specified number of knots, placed as to minimize the average distance between samples and knots (Lindgren, 2012 - Fig. SI.1). Thus, all the points nearest to a particular knot belong to the same cell, and crabs within each cell are assumed to be homogenous and evenly mixed, such that every sample location s_i within cell s has the same density, fishing mortality, recruitment, process error, etc. Cell s has area denoted by area_s (in units km^2) and all the data inputs and model outputs are indexed by those cells s . The SPDE approach thus approximates a smooth spatial surface in a computationally efficient way, and is common in spatial analyses (Thorson, 2019; Cao et al., 2020; Anderson et al., 2022). Mesh creation was performed via functionality in the R-INLA package (Lindgren, 2012).

2.3.3. Validation

Model convergence was assumed to have occurred if the absolute value of the final gradient of the marginal likelihood with respect to the fixed effects was <0.0001 for all parameters, and the Hessian matrix was positive definite. We checked model residuals and validated the model by using the DHARMA framework (Hartig, 2022) by computing QQ-plot residuals and plotting how residuals vary with magnitude of the predictions for both survey and fishery data. None of our diagnostics highlighted any strong patterns in the residuals and hence do not indicate any strong inconsistencies between the models and the data (Figs SI.9 and SI.10).

2.3.4. Derived quantities and ecological analysis

We explored the relative impact of fishing on the summer distribution across the EBS shelf by calculating exploitation rates by year, cell, and size-class as the ratio of catch and abundance, representing the exploitation rates at the time of the survey, which provides information about the spatial heterogeneity of fishing (Supp. Mat.SI). We also examined the potential influence of the cold pool on the spatial distribution of snow crabs by comparing the spatiotemporal variation in cold pool extent and abundance for all size classes and recruitment by extracting the locations of the top 95% of abundances across the spatial area studied (Supp. Mat. SI)

3. Results

3.1. Accounting for seasonal movement

Survey and catch data differed in terms of their centers of gravity (Fig. 2.a). Small size-classes (<40 mm and $40\text{--}78$ mm) were found in the northeastern part of the EBS in the middle shelf, whereas larger crabs ($78\text{--}101$ mm and >101 mm) were found in the middle of the EBS, on the edge between the middle and outer shelf. The co-occurrence of the COGs among size classes differed among years. For example, the centers of gravity were quite dispersed during 1995–1998 and 2007–2012 whereas they were in similar locations in the middle shelf during 2002–2006 and 2016–2018 (Fig. 2.b).

The centers of gravity of the observed catches were mostly distributed on the outer shelf in deeper waters. The spatial distribution of reconstituted catch strongly matches the spatial resolution of the survey abundance by size class (Fig. 2.a). Our results also highlight temporal variability in the distance between the COG of survey densities and catches (Fig. 2.b), with larger distances during 2006, 2007 and 2017 and shorter distances during 2012, 1989 and 2015. No relationship was found between cold pool extent and the distances between COGs for the

survey and the catches (Fig. SII.1).

3.2. Spatiotemporal changes in estimates of abundance

Estimates of abundance show notable temporal and spatial variation within and among size-classes. Size-class 1 exhibits high interannual variability (Fig. 4.a-d). Median abundances for size-classes 2, 3 and 4 declined consistently from the early 1989 to 2018 (Fig. 4). Local abundances at the end of the time series are estimated to be on average $\sim 90\%$, $\sim 63\%$, $\sim 60\%$ of the abundance at the end of the 1980s, for size-classes 2, 3, and 4 respectively. This pattern contrasts with the time-series of total abundance where total abundance is the highest at the end of the time-series for size-classes 1 and 3 (Fig. 4.a, c). Some cells have very high abundance compared to others (with a maximum ratio of 3.10^5 between the most and least abundant cells) (Fig. SII.2). The highest abundances for size-classes 1 and 2 are in the north of the EBS, in the middle and inner shelf while size-classes 3 and 4 are most abundant in the middle and outer shelf.

Through the pairwise correlation matrix the model estimated strong spatiotemporal correlation (> 0.5) between size-classes 2 and 3 (0.569) and between size-classes 3 and 4 (0.881) whereas size-class 1 had low and medium correlations, even with size-class 2 (0.29) (Fig. 4.e). Such low correlation is related to the high variability of recruitment compared with abundance in other size classes. By contrast, strong correlation for the larger size classes illustrates that individuals in these size classes are more likely to have similar spatial distributions.

3.2.1. Spatiotemporal changes in exploitable, mature, immatures abundances and recruitment

Estimated exploitable abundance showed marked spatiotemporal variability, with a consistent declining trend by a factor of 2 (natural scale) from the end of the 1990's to the 2018 (Fig. 5.a, d). Years with marked declines (1992–1994, 1999–2004, 2016–2018) in exploitable abundances (Fig. 5.d) were characterized by COG of exploitable abundances in the high latitudes (Fig. 5.b). In contrast, peaks in exploitable abundances (1991, 1998, 2014, 2015) occurred when COG of exploitable abundances were in the low latitudes.

Mature and immature abundances also showed marked spatiotemporal variability (Figs SII.3 and SII.4), with a consistent declining trend from the end of the 1990's to 2018. Median abundance at the end of the time-series was estimated to be $\sim 71\%$ and $\sim 52\%$ of the abundance at the end of the 1980s, for mature and immature respectively. Mature crabs are distributed in lower latitudes than immature crabs (Figs SII.3.a, SII.3.b and SII.4.a, SII.4.b). As previously observed for exploitable abundance, reductions in mature and immature crabs (2000–2004 and 2017–2018) are associated with distributional changes to high latitudes.

Recruitment showed a sporadic pattern temporally, with very high recruitment in 2008, 2012, 2015 (Fig. 6.a and d) when most of the recruits were found at the northern latitudes (Fig. 6.a and c) near the northern limit of the EBS.

3.3. Spatiotemporal changes in fishing mortality

Our modeling approach allowed us to estimate effective fishing mortality (i.e., how many crab were harvested at the survey timing and location) after translating winter catches to summer distribution. High estimated fishing mortalities (1989–1998, 2012–2015) were mostly associated with large areas with high harvests (almost all the EBS, Fig. 7.a) and with a COG of medium latitude within the EBS (Fig. 7.c,d). Size-class 4 represented 94% of the total catch. Years of low fishing mortality ($F \sim 0.08\text{yr}^{-1}$, 1999–2010) (Fig. 7.d) were associated with a more constrained spatial distribution of fishing mortality (for a given year more than 50% of the cells were not harvested, Fig. 7.a), and a northwestern COG of fishing mortality (Fig. 7.b and c).

From 1989 to 1998, the western part of the EBS had high exploitation rates (the average exploitation rate across space and time is 0.22; Fig. 8.

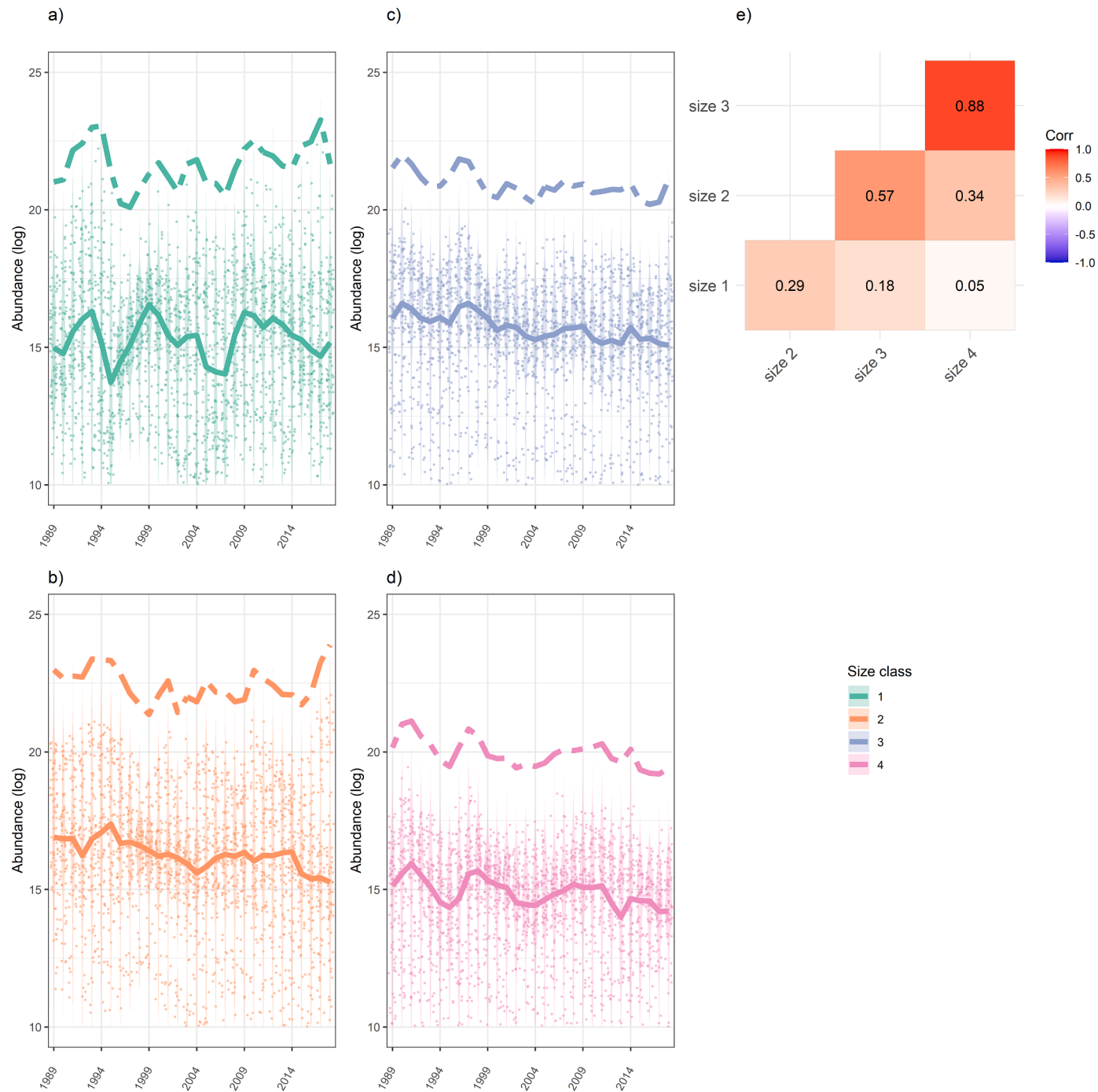


Fig. 4. Estimated abundances. (a-d) Time-series of estimated abundance for size classes 1–4. Thick lines are medians over space, dots represent the spatial variability (cells) for a given year and the dashed lines represent the total abundance (sum over cells). (e) Spatiotemporal covariation between size-classes.

a). After 1999, when the stock was declared overfished, exploitation rates declined markedly (to ~ 0.1 on average). The locally experienced exploitation rate can be drastically different than the exploitation rate for a spatially aggregated model (i.e., the one used in management, here ER_agg in Fig. 8.a). In some areas the catches represented 80% of the abundance whereas in other areas they represent 0% of the abundance (Fig. 8.a and b).

3.4. Potential drivers of the spatiotemporal variability of juveniles

For all size classes, low abundance (2003–2005, 2016–2018) was always associated with a weak cold pool extent (Fig. 9.a; SII.5.a, SII.6.a,

SII.7.a, SII.8.a). For size-classes 1 and 2, high abundances in 2007–2012 were associated with an extended cold pool area (Fig. 9.a, Fig. SII.6.a). The Pearson correlation between the time-series of abundance for size-class 1 and the cold pool extent was positive but not significant at the 5% level ($0.32, p = 0.065$). Also, the spatiotemporal distributions of the abundance of size-classes 1 and 2 during year $t + 1$ overlap with the cold pool of year t (Fig. 9.b). In warm years, the spatial distribution of abundance was more restricted, as is that of the cold pool (Fig. 9.b; Fig. SII.6.b). In contrast, the spatial distribution of the cold pool and abundance during cold years appeared to match and could extend over the entire EBS. However such spatial link with crab abundance and cold pool extent was not observed for size-classes 3, 4 and recruitment (Fig.

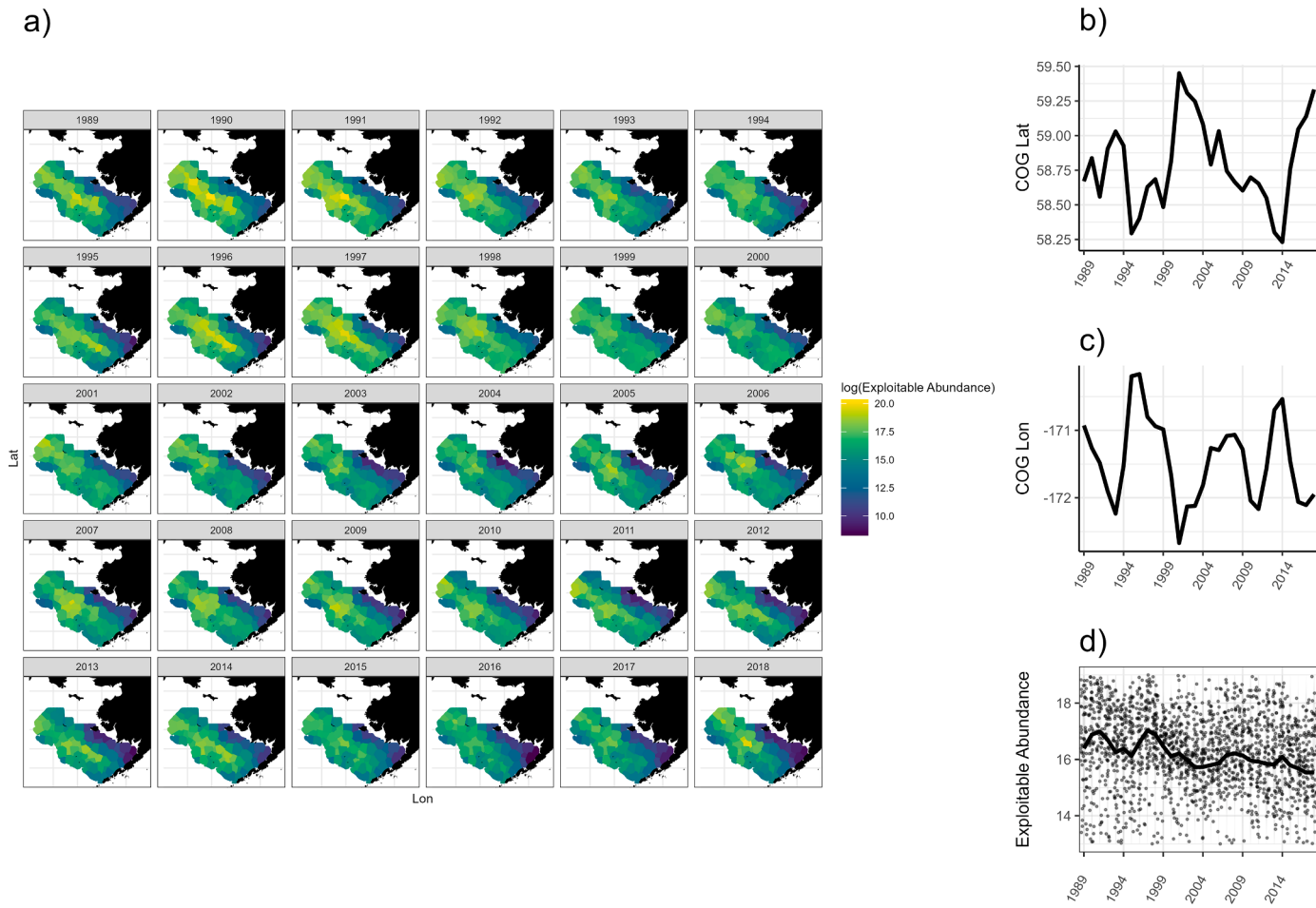


Fig. 5. Spatiotemporal variation in exploitable abundance (a). Time series of latitudinal (b) and longitudinal (c) variation in centers of gravity. (d) Temporal trend in exploitable abundance (thick line is the median and dots represent the spatial variability (knots) for a given year).

SII.5.b, Fig. SII.7.b, Fig. SII.8.b).

4. Discussion

Few spatial assessments have been used as the basis for management advice (Berger et al., 2017) and we consider our study as a step towards the integration of spatial dynamics into stock assessment. Based on previous work, we developed a size-structured spatiotemporal model to estimate fine-scale population dynamics and fishing impacts. Compared with previous studies which developed the conceptual basis of the framework and assessed its performance using simulations, this paper demonstrates the operational applicability of the framework and the critical points that need to be tackled when moving from simulations to case studies. Ultimately, the model provides estimates of spatiotemporal variation in key quantities, such as exploitable abundance, fishing mortality, recruitment, and mature and immature abundance. The model showed a decline in exploitable abundance and in fishing mortality, with the latter not evenly distributed. Results also show sporadic recruitment, spatially concentrated in the northeast part of the EBS. Finally, our results highlight that spatial distribution of juveniles is related to the cold pool.

4.1. Comparison with standard stock assessment methods

Some aspects of the model of this paper are substantially more complicated than those on which management advice is conventionally based. As such, it is able to document spatial changes in abundance and mortality (Figs. 5–8) and hence identify areas where exploitation rates

are spatially concentrated. The fine scale resolution of abundance would allow future work to explore effort dynamics, i.e. how vessels select the areas fished given a catch limit. A spatiotemporal model should also reduce bias caused by fishing mortality being spatially heterogeneous, leading to catch size-compositions not matching the size-composition of the underlying population. The problem is addressed within non-spatial models using time-varying selectivity (Nielsen and Berg, 2014) but at the cost of added model complexity.

Most stock assessment methods on which management advice is based either ignore spatial structure by treating differences in age- or size-structure spatially as a consequence of the effects of fishery or survey selectivity, or allow for spatial structure using a small number (<20) of areas within which population dynamics are modeled (Fourner et al., 1998; Begley and Howell, 2004; Bull, 2012; Methot and Wetzel, 2013; Doonan et al., 2016). However, neither of these approaches provide information on possible local depletion effects, which are often of interest to managers. The possibility of local depletion has been postulated for snow crab given the fishery is spatially concentrated (Parada et al., 2010). However, our results do not provide strong evidence for local depletion of snow crab. Continued monitoring of the results of spatiotemporal models to assess whether there is evidence for local depletion could be part of the management process.

The spatial estimates of exploitable abundance may also be used to assess the effects of bycatch of snow crab in fisheries other than the directed fishery, modeled here. Specifically, the bycatch of snow crab in fisheries targeting groundfish is low compared to the catch by the directed fishery but may be spatially concentrated relative to distribution of snow crab biomass. A spatiotemporal model could be used to

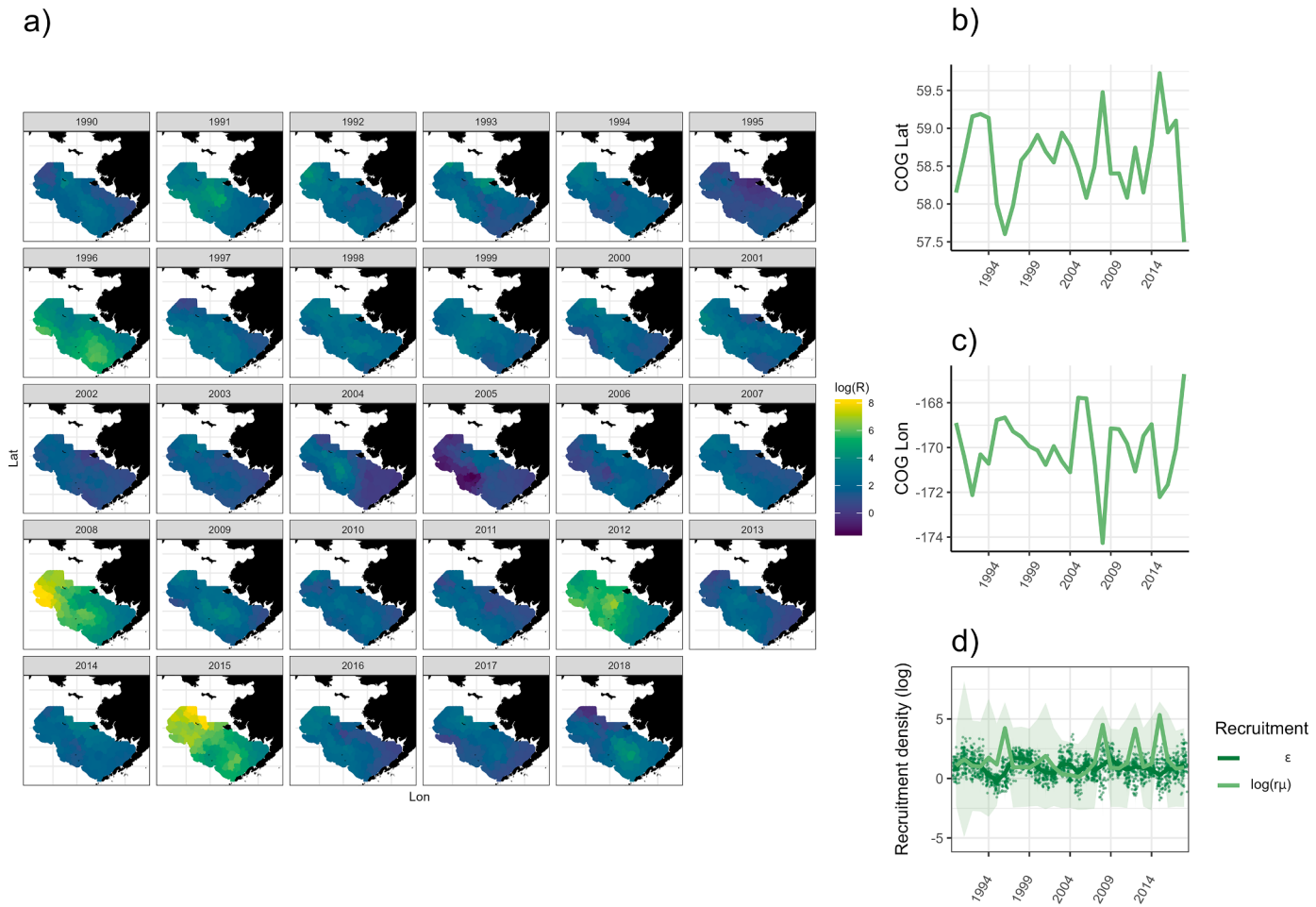


Fig. 6. Spatiotemporal variation in recruitment (a). Time series of latitudinal (b) and longitudinal (c) variation in centers of gravity. (d) Temporal trend in recruitment density. Light green dots and lines: $\log R_\mu$ represents the estimated recruitment (green shaded area represents the 95% confidence interval). Dark green dots and line: dots represent the spatial variability (knots) for a given year (i.e. process error for size class 1, $e_{t,s,l=1}$) and dark green line represents the temporal trend (median) of spatiotemporal variation in $e_{t,s,l=1}$.

identify spatial closures to reduce unintended bycatch, but the temporal resolution of the model would have to be re-evaluated and the linear translation of the catch to the time of the survey would no longer be a tenable strategy because bycatch occurs throughout the year.

4.2. Accounting for seasonal movement

A key feature of the snow crab is the differences in spatial distribution between summer and winter due to seasonal migration. We used an approach based on assigning spatial catches to spatial locations of the crabs that would have been caught because the model is defined on a yearly time step and no data were available to infer seasonal movement between summer (survey) and winter (fishery). The modeling of seasonal movement includes components for directional displacement (advection) as well as diffusive movement. An alternative approach would be to account for movement and seasonality within the modeling framework through some mechanistic approach. However, there is currently no basis for such an approach.

Some IPMs already account explicitly for seasons but implicitly for movement to infer interannual variation in phenology (e.g., Thorson et al., 2020) and seasonal changes in distribution (Gonzalez et al., 2021). Other population dynamics models have been developed using individual movement (advection-diffusion movement), but they account for seasonality implicitly (Thorson et al., 2017). More recently, analysts have developed explicit diffusion-taxis models based on a seasonal temporal resolution to explicitly model movement (e.g., Sibert et al.,

1999; Senina et al., 2020; Thorson et al., 2021). Fitting these types of model requires the specification of either: (1) a habitat-preference function based on small-scale tagging and experimental habitat-selection experiments, or (2) a range of hypothesized preference functions to bracket uncertainty when exploring model sensitivity to seasonal movement.

In our case, this would require additional data sources (e.g., movement data such as capture/recapture data) and, most of the time, stocks do not benefit from such data sources except when specific studies are designed to study movement (Thorson et al., 2021). Therefore, we argue that the actual framework (i.e., a model that does not account for movement through mechanistic equations but captures its effects through process error terms that are spatially correlated) remains the approach that is most likely to be applied given the data that are commonly available to fisheries scientists (i.e. spatialized survey data and catch data).

4.3. Accounting for process error

We used a state space approach, formulating the densities by size class in space to be latent states that are modeled with random effects correlated in space to account for process error. This formulation is analogous to single-species state-space models, where numbers at age are treated equivalently (Nielsen and Berg, 2014; Berg and Nielsen, 2016; Miller et al., 2016; Stock and Miller, 2021). A key difference compared to previous approaches to time variation is that there is no

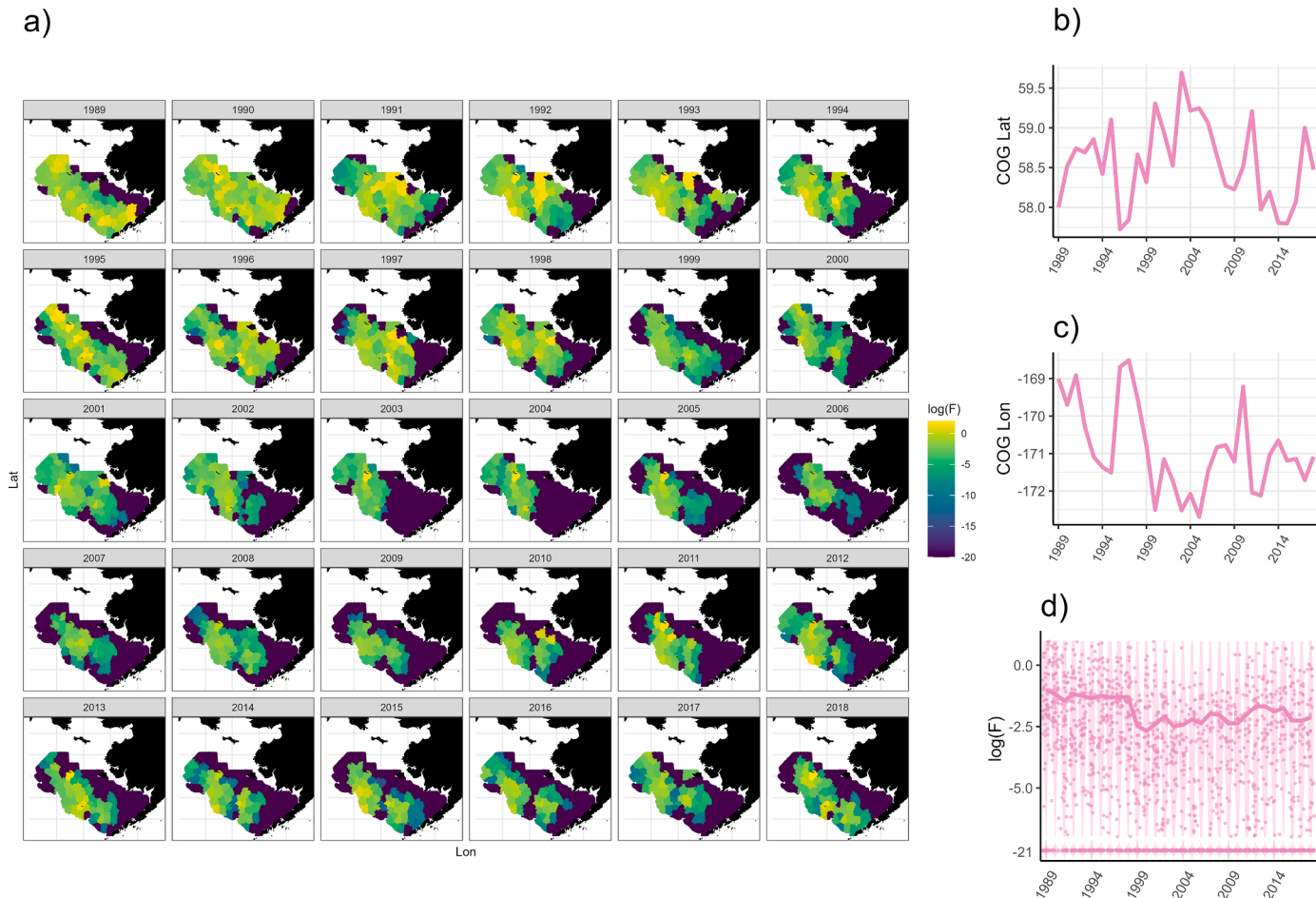


Fig. 7. Spatiotemporal variation in effective fishing mortality (F) (size-class 4) after translating the location of winter fishing to predict resulting summer impacts (a). Time series of latitudinal (b) and longitudinal (c) variation in centers of gravity. (d) Average temporal trend in fishing mortality (dots represent the spatial variability (knots) for a given year). Average time trend in fishing mortality was calculated as in Cao et al. (2020) when calculating fishing mortality for a spatially aggregated model. In both a) and d), value -21 represents 0 catch (in the log scale).

explicit structural link to a biological or physical quantities, such as when selectivity, catchability or natural mortality vary over time in a constrained way (Maunder, 2001; Methot and Wetzel, 2013). Instead, the model is given the flexibility to vary through time without any specific structure or constraint besides the hierarchical penalty-/structure and spatial correlation. Models such as those of Berg and Nielsen (2016) interpret the process error as mortality variation. Here we used this flexibility to explain patterns in the data that arise from some unmodelled (misspecified) spatiotemporal variation in biological (e.g., maturity, growth, movement and natural mortality) or observational process (e.g., selectivity) associated with specific size-classes.

This may seem to be an advantage of state-space models, because the model never matches reality and there are always un-modeled processes. But it can also lead to unpredictable behavior, particularly when there are data sources in conflict, or important structural components of the model that are misspecified. Specifically, state-space models may be so flexible they can fit to the data even when grossly misspecified, and the results will not be meaningful for management, despite ostensibly fitting the data well. There are some studies evaluating the statistical behavior of single-species state-space models varying types of misspecification using simulation-estimation (e.g., Stock and Miller (2021)), but more research is needed to better understand the properties of these models in the stock assessment context. Our approach extends the state-space formulation to space and this extra layer of complexity will require tailored research to establish best practices. Until then, we argue this model provides some key advantages

to existing approaches, but we recommend caution with formulation, fitting, and interpretation before consideration for use in tactical management (Auger-Méthé et al., 2021).

There are several other areas for further development. These include adding more data sources so that some of the currently pre-specified parameters can be estimated (e.g., bycatch in the groundfish fishery, results for other surveys and data on growth increments), including environmental drivers of recruitment and growth directly into the model framework as covariates associated with some of the parameters. Different drivers could be linked to each stage given the underlying hypotheses.

4.4. Population dynamics and the cold pool extent

The current analysis suggests there are links between the cold pool extent and the abundance of size-classes 1 and 2. Some literature emphasizes that the cold pool could be an important driver of spatial population structure for snow crab in the EBS (e.g., Muter and Litzow, 2008) and various mechanisms linking recruitment to the extent of the cold pool have been hypothesized: temperature can affect growth (Orensan et al., 2004, 2007), the length of the brooding period (Moriyasu and Lanteigne, 1998), settlement patterns, migration (Ernst et al., 2005, 2012), food availability, time in the pelagic phase (Kon, 1970; Szuwalski and Punt, 2013) and predation (Burgos et al., 2013). Recruitment and early life stages could be associated with the cold pool because of stenothermy of early benthic stages (Dionne et al., 2003;

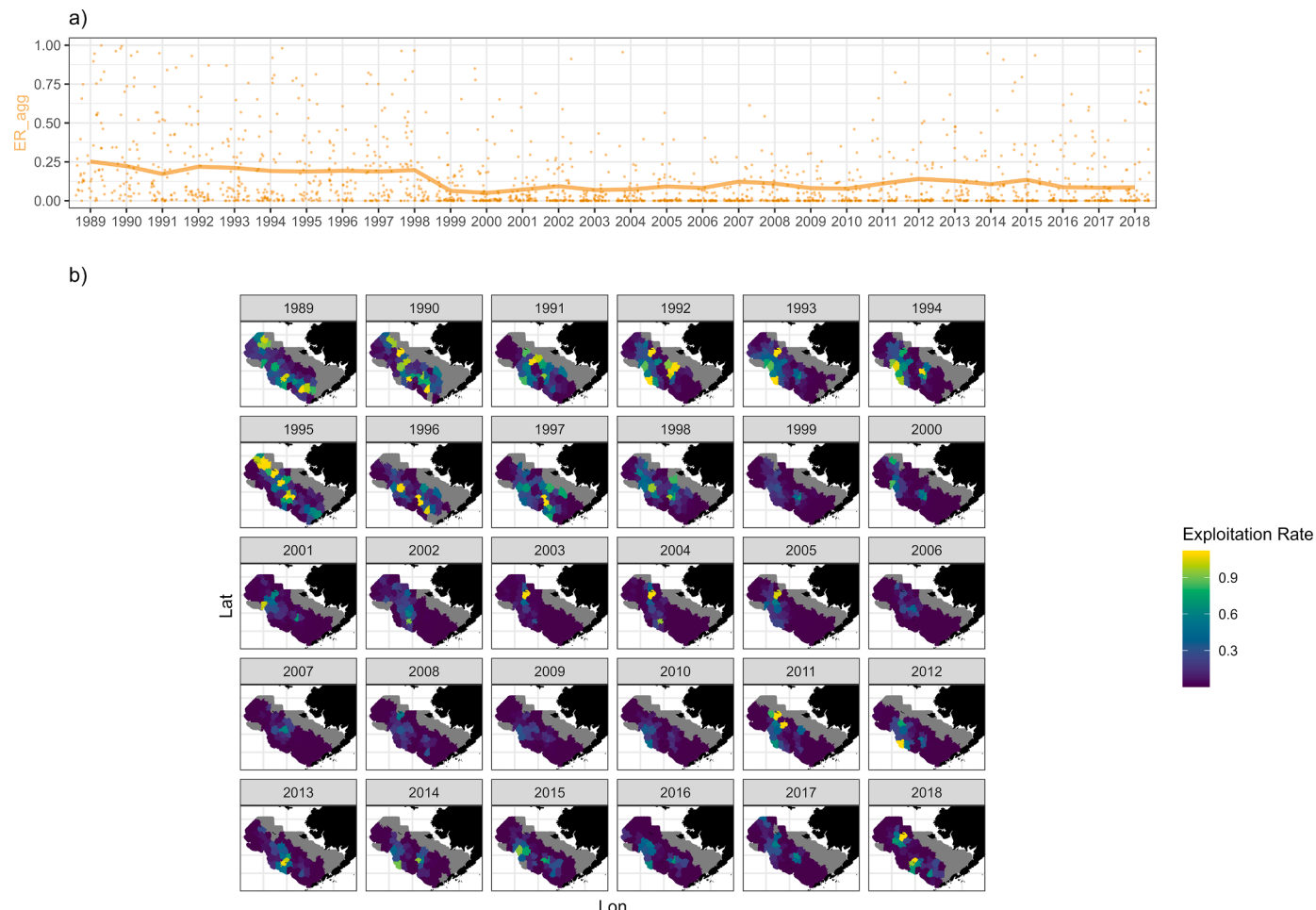


Fig. 8. Spatiotemporal variation in exploitation rate. a) Reconstructed exploitation rate for a spatially aggregated model (thick line, Eq.SI.18) for size-class 4; dots represent the spatial variability (knots) for a given year from the spatially explicit model (corresponding to panel b). b) Spatiotemporal variation in effective exploitation rate for size-class 4 after translating the location of winter fishing to predict resulting summer impacts.

(Orensanz et al., 2004). However, stenothermy is unlikely to explain the variability in snow crab spatial distribution and it has been hypothesized that fish predation, mostly by small Pacific cod (*Gadus macrocephalus*) might be one of the main sources of mortality for snow crab (Livingston, 1989). A potential underlying mechanism is that the cold pool acts as a thermal barrier to Pacific cod and imposes a spatial mismatch between the distributions of Pacific cod and juvenile crab. Consequently, during warm years the lack of a cold pool may remove the thermal barrier to cod predation, which might lead to contraction of the distribution of juvenile crab to the north of the EBS (Orensanz et al., 2004; Burgos et al., 2013). Alternatively, movement out of the model domain could explain the lower recruitment during 2000–2004 and 2017–2018 (warm years in the EBS). Our correlative approach is not sophisticated enough to test these alternative hypotheses, but future work could investigate further these processes to evidence their effect on population dynamics (Maunder and Deriso, 2011).

4.5. Future work: moving towards an MSE

The model could form the basis for the operating model component of a management strategy evaluation (MSE; Punt et al., 2016) that would be able to capture fine-scale movement, mortality and growth dynamics and also fleet dynamics. These aspects are usually ignored in the management strategies used to manage fisheries in the USA. An MSE based on a spatiotemporal operating model could quantify the consequences of using a simple assessment method for management advice. Such a model

could also assess the benefits and costs associated with moving management to incorporate spatial management more completely, specifically by regulating the distribution of fishing effort to make fishery mortality more homogenous spatially. The spatiotemporal model would need to be augmented with a model for effort dynamics with a better representation of seasonality as our model has focused only on summer survey timing, whereas the snow crab fishery and its management take place during winter. The model should also take better account of how movements, mortality, growth and maturation are likely to evolve in the future.

Authors' contributions

CS, AEP and JTT conceptualized this project and conceived the ideas. MO conceptualized this project in term of evolution of overarching research goals and aims. MO, CS, AEP, JTT, JC designed methodology. MO pre-processed subsets of data; MO wrote the code and adjusted JC code and analyzed the data. MO led the writing of the manuscript. CCM helped with model checking. MO, CS, AEP, JTT, JC, CCM, BA contributed critically to the drafts and gave final approval for publication.

Declaration of Competing Interest

The authors declare that they have no known competing financial interests or personal relationships that could have appeared to influence the work reported in this paper.

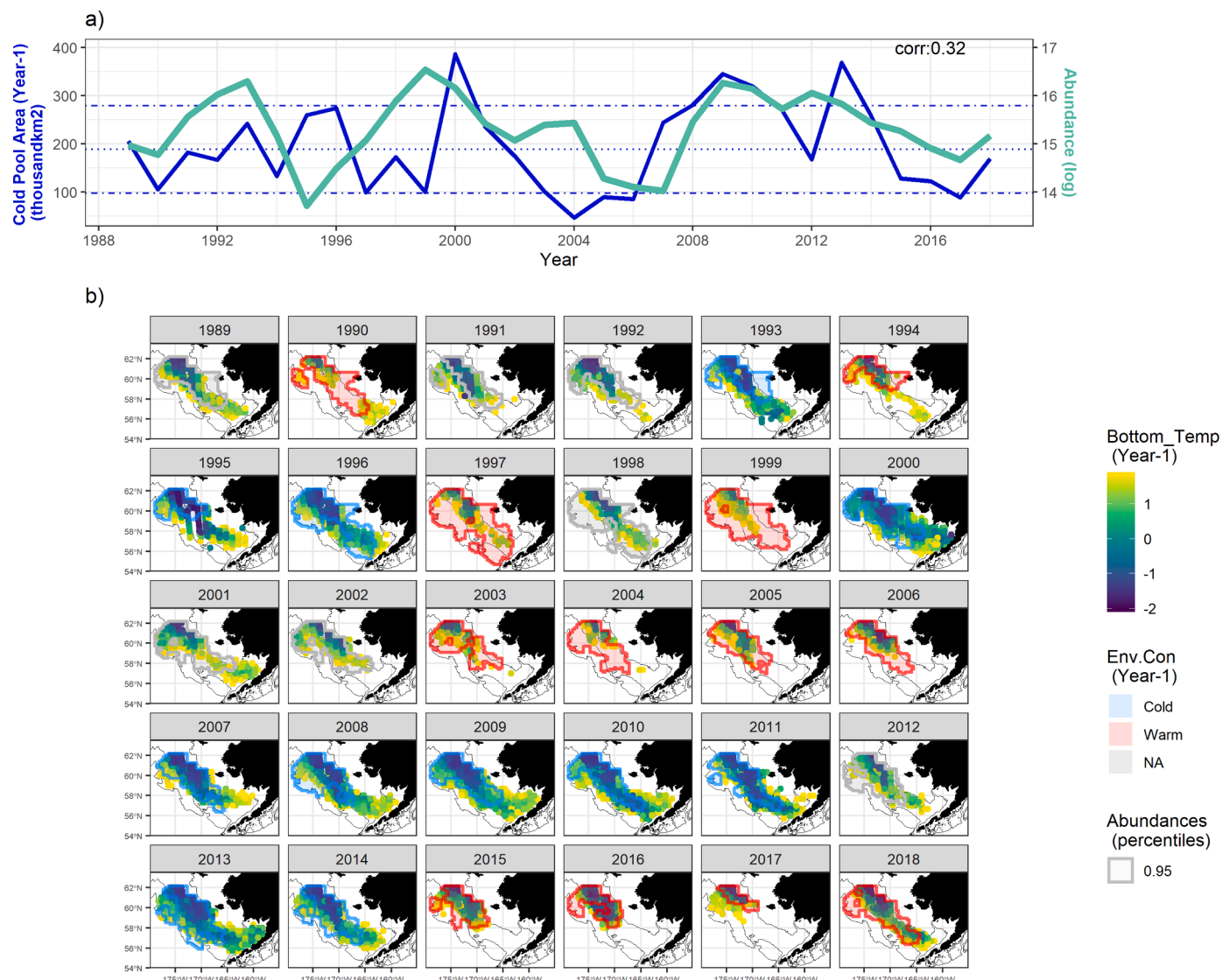


Fig. 9. Spatiotemporal variation in cold pool extent and the abundance of size-class 1. (a) Time series of cold pool extent (1 year lag) and temporal trend (median) in size-class 1 abundance. (b) Spatial distribution of the cold pool (1 year lag), and 95% percentiles of abundances for size-class 1 when environmental conditions (1-year lag) are considered as cold (blue) or warm (red).

Data availability

All data are presented and provided in Supp.Mat.I. Survey data are available via <https://www.fisheries.noaa.gov/alaska/commercial-fishing/alaska-groundfish-bottom-trawl-survey-data>. Fishery data are property of the Alaska Department of Fish and Game and should be requested through the Federal Agency ben.daly@alaska.gov.

Acknowledgements

We thank the many scientists (RACE NOAA division of the Alaska Fisheries Center) who have worked long hours to provide survey data for the eastern Bering Sea. We also thank Ben Daly from ADFG for providing the spatial fishery catch, and the NPFMC Crab Plan Team for providing feedback on snow crab biology. This publication was partially funded by the Cooperative Institute for Climate, Ocean, & Ecosystem Studies (CICOES) under NOAA Cooperative Agreement NA15OAR4320063. The authors also thank Eric Ward and two anonymous reviewers whose feedback greatly improved the manuscript.

Supplementary materials

All the Supplementary material documents are available at the Ecological Modelling online version of the manuscript. They provide additional information on the modeling framework (model, data, parameters, fit to data) (Supp. Mat. I) and results (Supp. Mat. II). Supplementary material associated with this article can be found, in the online version, at [doi:10.1016/j.ecolmodel.2023.110484](https://doi.org/10.1016/j.ecolmodel.2023.110484).

References

- Anderson, S.C., Ward, E.J., English, P.A., Barnett, L.A.K., 2022. sdmTMB: an R package for fast, flexible, and user-friendly generalized linear mixed effects models with spatial and spatiotemporal random fields. preprint Ecology. <http://biorxiv.org/lookup/doi/10.1101/2022.03.24.485545>. Accessed 29 March 2022.
- Auger-Méthé, M., Newman, K., Cole, D., Empacher, F., Gryba, R., King, A.A., Leos-Barajas, V., et al., 2021. A guide to state-space modeling of ecological time series. *Ecol. Monogr.* 91, e01470.
- Barbeaux, S.J., Hollowed, A.B., 2018. Ontogeny matters: climate variability and effects on fish distribution in the eastern Bering Sea. *Fish. Oceanogr.* 27, 1–15.
- Begley, J., Howell, D., 2004. An overview of gadget, the globally applicable area-disaggregated general ecosystem toolbox. *ICES CM 2004/FF 13*.
- Berg, C.W., Nielsen, A., 2016. Accounting for correlated observations in an age-based state-space stock assessment model. *ICES J. Mar. Sci.* 73, 1788–1797.

- Berger, A.M., Goethel, D.R., Lynch, P.D., Quinn, T., Mormede, S., McKenzie, J., Dunn, A., 2017. Space oddity: the mission for spatial integration. *Canad. J. Fish. Aquat. Sci.* 74, 1698–1716.
- Bull, B. 2012. CASAL (C++ algorithmic stock assessment laboratory) CASAL User Manual v2.30-2012/03/2: 282.
- Brevik, O.N., Aanes, F., Søvik, G., Aglen, A., Mehl, S., Johnsen, E., 2021. Predicting abundance indices in areas without coverage with a latent spatio-temporal Gaussian model. *ICES J. Mar. Sci.* 78, 2031–2042.
- Burgos, J., Ernst, B., Armstrong, D., Orensanz, J.(Lobo), 2013. Fluctuations in range and abundance of snow crab (*Chionoecetes opilio*) from the Eastern Bering Sea: what role for Pacific Cod (*Gadus macrocephalus*) predation? *Bull. Mar. Sci.* 89, 57–81.
- Cadigan, N.G., Wade, E., Nielsen, A., 2017. A spatiotemporal model for snow crab (*Chionoecetes opilio*) stock size in the southern Gulf of St. Lawrence. *Canad. J. Fish. Aquat. Sci.* 74, 1808–1820.
- Cadrin, S.X., 2020. Defining spatial structure for fishery stock assessment. *Fish. Res.* 221, 105397.
- Cao, J., Thorson, J.T., Punt, A.E., Szuwalski, C., 2020. A novel spatiotemporal stock assessment framework to better address fine-scale species distributions: development and simulation testing. *Fish. Fish.* 21, 350–367.
- Dionne, M., Sainte-Marie, B., Bourget, E., Gilbert, D., 2003. Distribution and habitat selection of early benthic stages of snow crab *Chionoecetes opilio*. *Mar. Ecol. Prog. Ser.* 259, 117–128.
- Doonan, I., Large, K., Dunn, A., Rasmussen, S., Marsh, C., Mormede, S., 2016. Casal2: new Zealand's integrated population modeling tool. *Fish. Res.* 183, 498–505.
- Edwards, A.M., Auger-Méthé, M., 2019. Some guidance on using mathematical notation in ecology. *Methods Ecol. Evol.* 10, 92–99.
- Ernst, B., Orensanz, J.(Lobo), Armstrong, D.A., 2005. Spatial dynamics of female snow crab (*Chionoecetes opilio*) in the eastern Bering Sea. *Canad. J. Fish. Aquat. Sci.* 62, 250–268.
- Ernst, B., Armstrong, D.A., Burgos, J., Orensanz, J.M.(Lobo), 2012. Life history schedule and periodic recruitment of female snow crab (*Chionoecetes opilio*) in the eastern Bering Sea. *Canad. J. Fish. Aquat. Sci.* 69, 532–550.
- Fokkema, W., van der Jeugd, H.P., Lameris, T.K., Dokter, A.M., Ebbing, B.S., de Roos, A. M., Nolet, B.A., et al., 2020. Ontogenetic niche shifts as a driver of seasonal migration. *Oecologia* 193, 285–297.
- Fournier, D.A., Hampton, J., Sibert, J.R., 1998. MULTIFAN-CL: a length-based, age-structured model for fisheries stock assessment, with application to South Pacific albacore, *Thunnus alalunga*. *Canad. J. Fish. Aquat. Sci.* 55, 2105–2116.
- Gaeuman, W.B., 2014. Summary of the 2013/2014 mandatory crab observer program database for the Bering Sea/Aleutian Islands commercial crab fisheries. Alaska Department of Fish and Game, Fishery Dataseries No.14-49, Anchorage.
- Goethel, D.R., Quinn, T.J., Cadrin, S.X., 2011. Incorporating spatial structure in stock assessment: movement modeling in marine fish population dynamics. *Rev. Fish. Sci.* 19, 119–136.
- Hartig, F. DHARMA: Residual Diagnostics for Hierarchical (Multi-Level / Mixed) Regression Models. R package version 0.4.6. <https://cran.r-project.org/web/packages/DHARMA/index.html>.
- Hilborn, R., Walters, C.J., 1992. Quantitative Fisheries Stock assessment: choice, Dynamics and Uncertainty. Springer, Dordrecht, p. 570.
- Kon, T., 1970. Fisheries biology of the Tanner crab, the duration of planktonic stages estimated by rearing experiments of larvae. *Nippon Suisan Gakkaishi* 36, 219–224.
- Kristensen, K., Nielsen, A., Berg, C.W., Skaug, H., Bell, B.M., 2016. TMB: Automatic Differentiation and Laplace Approximation. *J. Stat. Softw.* 70, 05.
- Kristensen, K., Thygesen, U.H., Andersen, K.H., Beyer, J.E., 2014. Estimating spatio-temporal dynamics of size-structured populations. *Canad. J. Fish. Aquat. Sci.* 71, 326–336.
- Kruse, G.H., Tyler, A.V., Sainte-Marie, B., Pengilly, D., 2007. A workshop on mechanisms affecting year-class strength formation in snow crabs *Chionoecetes opilio* in the eastern Bering Sea. *Res. Bull.* 12 (278–291), 16.
- Lindgren, F., Rue, H., Lindström, J., 2011. An explicit link between Gaussian fields and Gaussian Markov random fields: the stochastic partial differential equation approach: link between Gaussian Fields and Gaussian Markov Random Fields. *J. Royal Stat. Soc. Series B (Statistical Methodology)* 73, 423–498.
- Lindgren, F., 2012. Continuous domain spatial models in R-INLA. *ISBA Bull.* 19 (14–20), 8.
- Livingston, P.A., 1989. Interannual trends in pacific cod (*Gadus macrocephalus*) predation on three commercially important crab species in the Eastern Bering Sea. *Fish. Bull.* 87, 807–827.
- Martin Gonzalez, G., Wiff, R., Marshall, C.T., Cornulier, T., 2021. Estimating spatio-temporal distribution of fish and gear selectivity functions from pooled scientific survey and commercial fishing data. *Fish. Res.* 243, 106054.
- Maunder, M.N., 2001. A general framework for integrating the standardization of catch per unit of effort into stock assessment models. *Canad. J. Fish. Aquat. Sci.* 58, 795–803.
- Maunder, M.N., Deriso, R.B., 2011. A state-space multistage life cycle model to evaluate population impacts in the presence of density dependence: illustrated with application to delta smelt (*Hypomesus transpacificus*). *Canad. J. Fish. Aquat. Sci.* 68, 1285–1306.
- Maunder, M.N., Punt, A.E., 2013. A review of integrated analysis in fisheries stock assessment. *Fish. Res.* 142, 61–74.
- McDonald, R.R., Keith, D.M., Sameoto, J.A., Hutchings, J.A., Flemming, J.M., 2021. Explicit incorporation of spatial variability in a biomass dynamics assessment model. *ICES J. Mar. Sci. fsab192*.
- Methot, R.D., Wetzel, C.R., 2013. Stock synthesis: a biological and statistical framework for fish stock assessment and fishery management. *Fish. Res.* 142, 86–99.
- Miller, T.J., Hare, J.A., Alade, L.A., 2016. A state-space approach to incorporating environmental effects on recruitment in an age-structured assessment model with an application to southern New England yellowtail flounder. *Canad. J. Fish. Aquat. Sci.* 73, 1261–1270.
- Moriyasu, M., Lanteigne, C., 1998. Embryo development and reproductive cycle in the snow crab, *Chionoecetes opilio* (Crustacea: majidae), in the southern Gulf of St. Lawrence, Canada. *Canad. J. Zool.* 76, 2040–2048.
- Mueter, F.J., Litzow, M.A., 2008. Sea ice retreat alters the biogeography of the Bering Sea continental shelf. *Ecol. Appl.* 18, 309–320.
- Nielsen, A., Berg, C.W., 2014. Estimation of time-varying selectivity in stock assessments using state-space models. *Fish. Res.* 158, 96–101.
- Orensanz, J.M., Ernst, B., Stabeno, P., and Livingston, P. 2004. Contraction of the geographic range of distribution of snow crab (*Chionoecetes opilio*) in the eastern Bering Sea: an environmental ratchet, 45:65: 79.
- Orensanz, J.M., Ernst, B., Armstrong, D.A., 2007. Variation of Female Size and Stage at Maturity in Snow Crab (*Chionoecetes opilio*) (Brachyura: majidae) from the Eastern Bering Sea. *J. Crustacean Biol.* 27, 576–591.
- Parada, C., Armstrong, D.A., Ernst, B., Hinckley, S., Orensanz, J.M., 2010. Spatial dynamics of snow crab (*Chionoecetes opilio*) in the eastern Bering Sea—Putting together the pieces of the puzzle. *Bull. Mar. Sci.* 86, 413–437.
- Punt, A.E., Butterworth, D.S., de Moor, C.L., De Oliveira, J.A.A., Haddon, M., 2016. Management strategy evaluation: best practices. *Fish. Fish.* 17, 303–334.
- Punt, A.E., 2019. Spatial stock assessment methods: a viewpoint on current issues and assumptions. *Fish. Res.* 213, 132–143.
- Punt, A.E., Dunn, A., Elvarsson, B.P., Hampton, J., Hoyle, S.D., Maunder, M.N., Methot, R.D., et al., 2020. Essential features of the next-generation integrated fisheries stock assessment package: a perspective. *Fish. Res.* 229, 105617.
- Quinn, T.J., Deriso, R.B., 1999. Quantitative Fish dynamics. Biological resource Management Series. Oxford University Press, New York, p. 542.
- Rogers, L.A., Storvik, G.O., Knutsen, H., Olsen, E.M., Stenseth, N.C., 2017. Fine-scale population dynamics in a marine fish species inferred from dynamic state-space models. *J. Anim. Ecol.* 86, 888–898.
- Senina, I., Lehodey, P., Sibert, J., Hampton, J., 2020. Integrating tagging and fisheries data into a spatial population dynamics model to improve its predictive skills. *Canad. J. Fish. Aquat. Sci.* 77, 576–593.
- Sibert, J.R., Hampton, J., Fournier, D.A., Bills, P.J., 1999. An advection-diffusion-reaction model for the estimation of fish movement parameters from tagging data, with application to skipjack tuna (*Katsuwonus pelamis*). *Canad. J. Fish. Aquat. Sci.* 56, 925–938.
- Stock, B.C., Miller, T.J., 2021. The Woods Hole Assessment Model (WHAM): a general state-space assessment framework that incorporates time- and age-varying processes via random effects and links to environmental covariates. *Fish. Res.* 240, 105967.
- Szuvialski, C., Punt, A.E., 2013. Regime shifts and recruitment dynamics of snow crab, *Chionoecetes opilio*, in the eastern Bering Sea. *Fish. Oceanogr.* 22, 345–354.
- Szuvialski, C., 2019. A Stock Assessment For the Eastern Bering Sea Snow crab, Stock Assessment and Fishery Evaluation Report for the King and Tanner Crab Fisheries of the Bering Sea and Aleutian Islands Regions. North Pacific Fishery Management Council, p. 350.
- Szuvialski, C., Cheng, W., Foy, R., Hermann, A.J., Hollowed, A., Holsman, K., Lee, J., et al., 2021. Climate change and the future productivity and distribution of crab in the Bering Sea. *ICES J. Mar. Sci.* 78, 502–515.
- Szuvialski, C.S., Punt, A.E., 2015. Can an aggregate assessment reflect the dynamics of a spatially structured stock? Snow crab in the eastern Bering Sea as a case study. *Fish. Res.* 164, 135–142.
- Thorson, J.T., Ianelli, J.N., Munch, S.B., Ono, K., Spencer, P.D., 2015. Spatial delay-difference models for estimating spatiotemporal variation in juvenile production and population abundance. *Canad. J. Fish. Aquat. Sci.* 72, 1897–1915.
- Thorson, J.T., Jannot, J., Somers, K., 2017. Using spatio-temporal models of population growth and movement to monitor overlap between human impacts and fish populations. *J. Appl. Ecol.* 54, 577–587.
- Thorson, J.T., 2018. Three problems with the conventional delta-model for biomass sampling data, and a computationally efficient alternative. *Canad. J. Fish. Aquat. Sci.* 75, 1369–1382.
- Thorson, J.T., 2019. Guidance for decisions using the Vector Autoregressive Spatio-Temporal (VAST) package in stock, ecosystem, habitat and climate assessments. *Fish. Res.* 210, 143–161.
- Thorson, J.T., Adams, C.F., Brooks, E.N., Eisner, L.B., Kimmel, D.G., Legault, C.M., Rogers, L.A., et al., 2020. Seasonal and interannual variation in spatio-temporal models for index standardization and phenology studies. *ICES J. Mar. Sci.* 77, 1879–1892.
- Thorson, J.T., Barbeaux, S.J., Goethel, D.R., Kearney, K.A., Laman, E.A., Nielsen, J.K., Siske, M.R., et al., 2021. Estimating fine-scale movement rates and habitat preferences using multiple data sources. *Fish. Fish.* faf.12592.
- Walters, C.J., Martell, S.J.D., 2004. Fisheries Ecology and Management. Princeton University Press, Princeton, N.J., p. 399.
- Zacher, L.S., Richar, J.I., and Litzow, M.A. 2021. The 2021 Eastern Bering Sea continental shelf trawl survey: results for commercial crab species: 193.